Published in "The Plant Journal 64(3): 470–481, 2011"
which should be cited to refer to this work.

The *PAM1* gene of petunia, required for intracellular accommodation and morphogenesis of arbuscular mycorrhizal fungi, encodes a homologue of VAPYRIN

Nadja Feddermann[1,†], Rajasekhara Reddy Duvvuru Muni[1,†,‡], Tatyana Zeier[1], Jeroen Stuurman[2], Flavia Ercolin[1], Martine Schorderet[1] and Didier Reinhardt[1,*]
[1]*Department of Biology, University of Fribourg, CH-1700 Fribourg, Switzerland, and*
[2]*Keygene NV, PO Box 216, 6700AE Wageningen, the Netherlands*

[‡]Present address: Samuel Roberts Noble Foundation, Ardmore, OK 73401, USA.

SUMMARY

Most terrestrial plants engage into arbuscular mycorrhizal (AM) symbiosis with fungi of the phylum *Glomeromycota*. The initial recognition of the fungal symbiont results in the activation of a symbiosis signalling pathway that is shared with the root nodule symbiosis (common *SYM* pathway). The subsequent intracellular accommodation of the fungus, and the elaboration of its characteristic feeding structures, the arbuscules, depends on a genetic programme in the plant that has recently been shown to involve the *VAPYRIN* gene in *Medicaco truncatula*. We have previously identified a mutant in *Petunia hybrida*, *penetration and arbuscule morphogenesis 1* (*pam1*), that is defective in the intracellular stages of AM development. Here, we report on the cloning of *PAM1*, which encodes a VAPYRIN homologue. PAM1 protein localizes to the cytosol and the nucleus, with a prominent affinity to mobile spherical structures that are associated with the tonoplast, and are therefore referred to as tonospheres. In mycorrhizal roots, tonospheres were observed in the vicinity of intracellular hyphae, where they may play an essential role in the accommodation and morphogenesis of the fungal endosymbiont.

Keywords: symbiosis, *Glomus intraradices, Petunia hybrida, VAPYRIN*, arbuscular mycorrhiza, ankyrin, intracellular accommodation.

INTRODUCTION

In arbuscular mycorrhizal (AM) symbiosis, the fungal partner penetrates the root and invades the epidermal and cortical cells of the plant host. This intimate interaction relies on the specific recognition of the endosymbiont, and requires a calcium-related symbiosis signalling cascade in the plant, the common SYM pathway, which is shared with the root nodule symbiosis (Oldroyd and Downie, 2006; Parniske, 2008; Oldroyd *et al.*, 2009). The common SYM pathway consists of at least eight genetically defined components (common *SYM* genes), which are functionally conserved among angiosperms (Gutjahr *et al.*, 2008; Markmann *et al.*, 2008), indicating that their origin pre-dates the divergence between monocots and dicots. Upon activation of the common SYM pathway a cellular accommodation programme of the plant host triggers the formation of an infection structure, the prepenetration apparatus (PPA), which guides the fungus through the lumen of root epidermal cells (Genre *et al.*, 2005), and later into cortical cells where arbuscules are formed (Genre *et al.*, 2008). The initial stages of arbuscule formation are associated with a dramatic reorganization of the host cell, involving virtually all cellular components, in particular the cytoskeleton, the nucleus, and the membrane system (Bonfante-Fasolo, 1984; Genre and Bonfante, 1998, 1999; Blancaflor *et al.*, 2001; Genre *et al.*, 2008). A central feature of colonized cortex cells is their periarbuscular membrane (PAM), which controls nutrient transfer between the symbiotic partners (Bucher, 2007).

In contrast to the well-characterized common SYM pathway, little is known about the molecular components involved in cellular rearrangement and the intracellular

accommodation of AM fungi. We have previously identified the *Petunia hybrida* mutant *penetration and arbuscule morphogenesis 1* (*pam1*) that exhibits strong resistance to AM fungal infection (Sekhara Reddy *et al.*, 2007). Whereas penetration of epidermal and cortical cells was frequently observed in *pam1* mutants, fungal hyphae formed aberrant intracellular structures and were often arrested and aborted. Hence, *pam1* mutants are compromised in intracellular accommodation of the fungus, but not in cellular invasion *per se*. A *Medicago truncatula* mutant with a similar phenotype has recently been shown to carry a mutation in a gene that was named *VAPYRIN* because of the composite structure of its gene product, which involves an N-terminal VAP domain and a C-terminal ankyrin domain (Pumplin *et al.*, 2010).

Here, we report the molecular identification of *PAM1*, which encodes a homologue of *VAPYRIN*. *PAM1* is induced during AM symbiosis, particularly in cells that harbour arbuscules. PAM1 protein was found to be cytosolic, with a prominent affinity to the spherical structures (tonospheres) that are associated with intracellular fungal hyphae. Besides *M. truncatula*, *PAM1* has homologues in many angiosperms, with the notable exception of the non-symbiotic species *Arabidopsis thaliana*, and in the moss *Physcomitrella patens*. Hence, *PAM1* may represent a component of an ancient cellular machinery that pre-dates the advent of vascular plants, and which became essential, during the course of the evolution of AM symbiosis, for intracellular accommodation and morphogenesis of the fungal endosymbiont.

RESULTS

Defects of *pam1-1* and *pam1-2* in arbuscule development and in symbiotic phosphate transporter gene expression

Establishment of AM symbiosis involves two intracellular stages: first the hyphal colonization of epidermal cells, and later the formation of arbuscules in cells of the root cortex. We have previously isolated the mutant *pam1-1* that exhibits defects at both intracellular stages (Sekhara Reddy *et al.*, 2007). Subsequently, an allelic mutant was isolated (*pam1-2*) that showed similar strong defects at epidermal and cortical stages of colonization when inoculated with soil inoculum containing spores and dried colonized roots. Under these conditions, roots of both mutant alleles were colonized only transiently, and the fungus was ultimately eliminated from the root system (Sekhara Reddy *et al.*, 2007), thus rendering detailed analysis of the cortical phenotype difficult. To address this issue, *pam1-1* and *pam1-2* mutants were inoculated with actively proliferating hyphal inoculum from well-colonized wild type plants (nurse plants). Because of the direct nutritional supply from the nurse plant, the strictly biotrophic fungus can potentially overcome early barriers in mutant roots, and therefore reveal subsequent aspects of the mutant phenotype.

Nurse plant inoculation resulted in the strong colonization of all three genotypes (Table 1). Intraradical colonization reached over 80% of the total root length in mutants as in the wild type, and hyphopodia were found in over 60% of the investigated root segments. However, arbuscule formation was significantly reduced in the mutants. Whereas arbuscular colonization reached 73% in the wild type, mutant roots did not contain any normal arbuscules, and only in 2–6% of the cases were strongly reduced branched intracellular structures observed in cortical cells (Table 1). Confocal microscopic analysis confirmed that the cortical cells of the mutant were indeed colonized, but that arbuscule development was arrested at an early point of branching (Figure 1a–c).

These findings raised the question of whether the residual intracellular colonization of cortical cells was associated with the induction of symbiosis-related functional markers. The best-characterized functional markers associated with arbuscule development are the symbiotic phosphate transporters (PTs) (Harrison *et al.*, 2002). Hence, we analysed the expression levels of the symbiosis-specific *PT4* of petunia (Wegmüller *et al.*, 2008) by quantitative real-time polymerase chain reaction (qRT-PCR). In mycorrhizal wild type plants, *PT4* was induced over 700-fold compared with controls (Table 2). In both mutant alleles, *PT4* was induced as well, but to much lower levels than in the wild type, and because of considerable variation, the induction was not statistically significant (Table 2). Taken together, these results show that *PAM1* is involved in both the regulation of arbuscule development and the induction of symbiotic *PT* expression.

Genetic analysis and cloning of *PAM1*

A cross between the homozygous stabilized *pam1-1* mutant (Sekhara Reddy *et al.*, 2007) and the unstable *pam1-2* allele resulted in 93.3% mutants (n = 105 F_1 plants) and 6.7%

Table 1 Mycorrhizal colonization of wild type plants and *pam1* mutants 4 weeks after inoculation from nurse plants

	Total intraradical[a]	Hyphopodia[a]	Arbuscules[b]
Wild type	86.0 ± 12.2	72.3 ± 10.7	73.3 ± 21.4
pam1-1	82.0 ± 2.65	64.3 ± 2.31	6.0 ± 4.36[c]
pam1-2	86.6 ± 3.06	70.6 ± 11.9	2.3 ± 1.53[c]

[a]These categories were not significantly different between mutant and wild type plants.
[b]The difference in arbuscular colonization between each mutant allele and the wild type was highly significant ($P < 0.001$), whereas the difference between the mutant alleles was not.
[C]arbuscules in *pam1* mutants never developed beyond early stages of branching, corresponding to the stages depicted in Figure 1b,c.
Colonization levels are expressed as percentages of the total root system (%).
Values represent the mean of three biological replicates ± standard deviations.

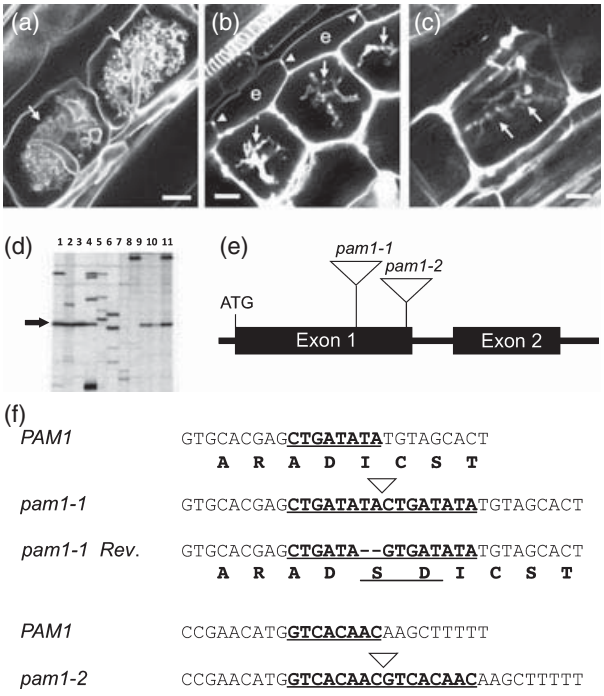

Figure 1. Symbiotic mutant phenotype and genetic analysis of *pam1* alleles. (a–c) Confocal microscopical analysis of mycorrhizal roots of the wild type (a), *pam1-1* (b) and *pam1-2* (c) stained with acid fuchsin. Arbuscules in the wild type are compact and finely branched, whereas mutants allow only for limited intracellular colonization, with just a few thin hyphae that are poorly branched (arrows). Endodermal cells (marked as e in panel b) can be identified by the staining of the Casparian strip (arrowheads).
(d) Transposon display revealed an amplicon (arrow) that co-segregated with the *pam1-2* phenotype. Lanes 1–11 represent DNA of the following genotypes: non-stable homozygous mutants (lanes 1–4), homozygous wild type (lanes 5–7), the parental *act*$^{-}$ line used for stabilization (lane 8), two stable heterozygous plants (lanes 9 and 10) and a stable mutant (lane 11).
(e) Organization of the *PAM1* gene with two exons and one intron. The position of transposon insertions in *pam1-1* and *pam1-2* is represented by triangles.
(f) Analysis of transposon insertion sites in *pam1-1* and *pam1-2*, and in a revertant progeny (*pam1-1 Rev*). Target site duplications are underlined and set in bold; positions of transposon insertions are indicated by triangles. The revertant allele derived from *pam1-1* has a restored reading frame with a 6-bp footprint, resulting in the insertion of two amino acids (SD) in the predicted protein sequence (see Figure 2). Scale bars: 10 μm.

revertants, with partially or completely restored symbiosis phenotypes. Phenotypic reversion in transposon-mutagenized populations can be explained by gene reversion as a result of transposon excision, and suggests that at least one of the *pam1* alleles is tagged by the transposon dTph1 (Gerats *et al.*, 1990). The transposon insertion responsible for the mutant phenotype was identified in a segregating population of *pam1-2* by transposon display (Figure 1d; Van den Broeck *et al.*, 1998). The *PAM1* gene consists of two exons and one intron (Figure 1e) and corresponds to a predicted open reading frame of 1608 nucleotides. As in the case of the *pam1-2* allele, which carries a dTph1 insertion at position 1056 from the predicted start codon, the *pam1-1* allele contains a transposon insertion at position 900 (Figure 1e). Both insertions are associated with an 8-bp target site duplication (Figure 1f), a typical feature of dTph1 insertions (Gerats *et al.*, 1990). Phenotypic wild type plants recovered from the cross between homozygous *pam1-1* and *pam1-2* carried a 6-bp footprint at the *pam1-1* insertion site (Figure 1f). This restores the open reading frame and results in an insertion of two amino acids (SD). Conceivably, this modification does not significantly change the tertiary structure of the protein (see below), hence allowing it to perform its wild type function in the revertant. The collective evidence described here strongly suggests that the transposon insertions in *PAM1* are the cause of the symbiosis mutant phenotypes in *pam1-1* and *pam1-2*.

Table 2 Expression of *PAM1* and *PT4* in wild type plants and *pam1* mutants 4 weeks after inoculation from nurse plants

	Control	*Glomus intraradices*
PAM1 in wild type	1[a] ± 0.34	2.01 ± 0.59
PAM1 in *pam1-1*	0.44 ± 0.14	0.61 ± 0.08
PAM1 in *pam1-2*	0.14 ± 0.02	0.49 ± 0.14[bc]
PT4 in wild type	1[a] ± 0.24	721.2 ± 289.1[b]
PT4 in *pam1-1*	0.362 ± 0.13	57.24 ± 10.45
PT4 in *pam1-2*	1.216 ± 1.32	42.98 ± 29.85

[a]Values of *PAM1* and *PT4* expression are indicated relative to *GAPDH*. Expression levels were normalized to 1 in non-mycorrhizal wild type plants.
[b]Induction of gene expression by *Glomus intraradices* was significant ($P < 0.05$).
[c]The difference of *PAM1* expression between *pam1-2* and wild type plants was significant.
Values represent the mean of three biological replicates ± standard deviations.

Structure and evolutionary conservation of the predicted PAM1 protein

The cDNA of *PAM1* is predicted to encode a protein of 535 amino acids. The N-terminal quarter (amino acids 1–134) contains a major sperm protein (MSP) domain (Figure 2a,b) that also occurs in VAMP-associated proteins (VAPs) (Lev *et al.*, 2008), and which has been implicated in interactions of plants with fungal pathogens (Laurent *et al.*, 2000). The C-terminal part of PAM1 consists of a large ankyrin domain with 11 ankyrin repeats (Figure 2a,b). Many of the canonical amino acids of the ankyrin repeats are conserved (Figure 2b). Ankyrin repeats are known to exhibit limited conservation at the level of the primary amino acid sequence, and yet, their three-dimensional structure is well conserved (Mosavi *et al.*, 2004). Although ankyrin repeats are widespread in eukaryotes, plant proteins with high numbers of ankyrin repeats (>10) have not been described to date. Three-dimensional modelling of the PAM1 domains revealed a β-sandwich organization for the MSP domain (Figure 2c) and a crescent-shaped ankyrin domain

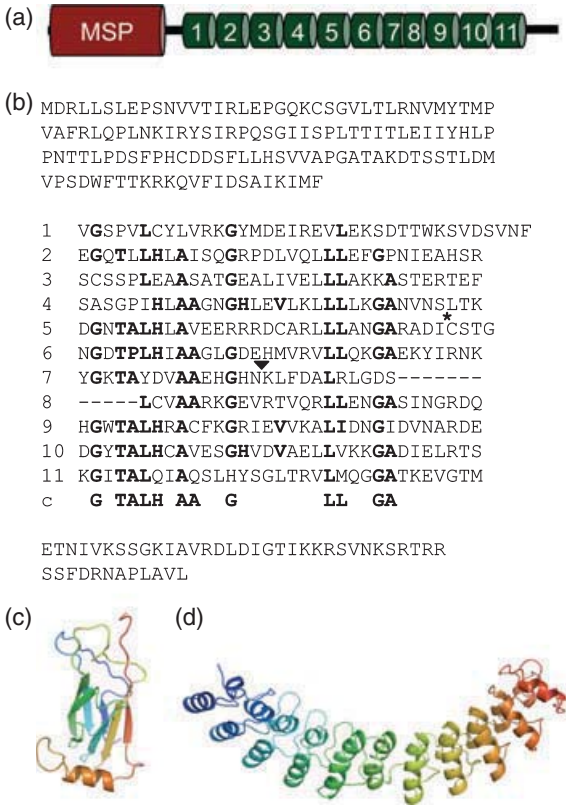

Figure 2. Analysis of the predicted PAM1 protein and its three-dimensional structure.
(a) Schematic representation of the primary PAM1 protein structure consisting of an N-terminal major sperm protein (MSP) domain and a C-terminal ankyrin repeat domain with 11 ankyrin repeats.
(b) Amino acid sequence of PAM1. The MSP domain (top four lines) is followed by 11 ankyrin repeats, of which two (seven and eight) are slightly truncated. Conserved residues are shown in bold. An asterisk indicates the position of the transposon insertion in *pam1-1* [and of a two-amino-acid insertion (SD) in the revertant allele; cf. Figure 1f]. An arrowhead indicates the transposon insertion in the *pam1-2* allele. The line below ankyrin repeat 11 highlights the consensus residues.
(c, d) Three-dimensional models of the MSP domain (c), and of the ankyrin domain (d). For clarity, the individual β-sheets were coloured in (c); in (d), each colour represents an individual ankyrin repeat.

(Figure 2d). The PAM1 ankyrin domain closely resembles the D34 domain of human ankyrin R (Mosavi *et al.*, 2004), which binds to integral membrane proteins in erythrocytes, and links them to the spectrin cytoskeleton (Bennett and Baines, 2001; Michaely *et al.*, 2002). The transposon insertions in *pam1-1* and *pam1-2* result in premature stop codons within the transposon sequence in ankyrin repeat 5 and 7, respectively (asterisk and arrowhead in Figure 2b).

Proteins composed of an MSP domain and an ankyrin domain are restricted to the plant kingdom. A closely related *PAM1* homologue was recently identified in *M. truncatula* (Pumplin *et al.*, 2010), and further homologues occur in the genomes of grape vine (*Vitis vinifera*), poplar (*Populus trichocarpa*), soybean (*Glycine max*), rice (*Oryza sativa*) and maize (*Zea mays*) (data not shown). Notably, the genome of the moss *P. patens* also contains a *PAM1* homologue, whereas no gene with a comparable domain structure was found in the *A. thaliana* genome, a non-mycorrhizal species.

Regulation of *PAM1* expression

To investigate the expression pattern of *PAM1* in the wild type, mRNA was extracted from various plant organs and reverse transcribed for analysis by qRT-PCR. Abundant levels of *PAM1* transcript were detected in the roots, whereas much lower, yet detectable, levels were found in shoot tips, stems, young leaves, mature leaves and flowers (Figure 3a). The roots of both mutant alleles exhibited lower, but significant, expression levels of *pam1* compared with wild type (Table 2). This residual expression is unlikely to reflect the expression of a related *VAPYRIN*-like gene, as found in the case of *M. truncatula* (Pumplin *et al.*, 2010), as similar results were obtained with independent primer sets amplifying 5′ and 3′ regions upstream and downstream of the intron and of both transposon insertions (see Experimental procedures). This indicates that the mutated mRNA is not subject to efficient non-sense-mediated mRNA decay (NMD), despite the introduction of premature stop codons within the sequence of dTPh1.

In order to assess the regulation of *PAM1* during AM symbiosis, mycorrhizal plants were sampled at different time points of symbiotic development up to 7 weeks after inoculation. *PAM1* expression in roots was induced during the AM interaction, in particular at the fully established stages of symbiosis from 29 days onwards (Figure 3b, top). Induction of *PAM1* in mycorrhizal roots was paralleled by the induction of *PT4*, which also peaked between 29 and 35 days after inoculation (Figure 3b, bottom).

PAM1 expression is induced in cells with arbuscules

To assess *PAM1* expression in mycorrhizal roots with cellular resolution, *in situ* hybridization experiments were carried out. In mock-inoculated plants, or in non-infected parts of colonized root systems, no expression above background level was detected (data not shown). Similarly, no *PAM1* expression was found in epidermal cells that were in contact with extraradical hyphae (Figure 4a). The establishment of the first hyphae in epidermal cells was associated with a moderate signal along the plant cytoplasmic sleeve that surrounds the invading fungal hypha (Figure 4b, arrow). Cells with contact to passing hyphae between the epidermis and the inner cortex (Figure 4c), and cells adjacent to growing hyphal tips (Figure 4d) did not express *PAM1* above background levels. However, elevated expression of *PAM1* was detected in cortical cells that contained arbuscules (Figure 4c,e, arrows). Notably, strong induction was observed only in a subset of cells with arbuscules. Confocal analysis revealed that a strong *PAM1* signal coincided with cells that contained dense, finely branched arbuscules with

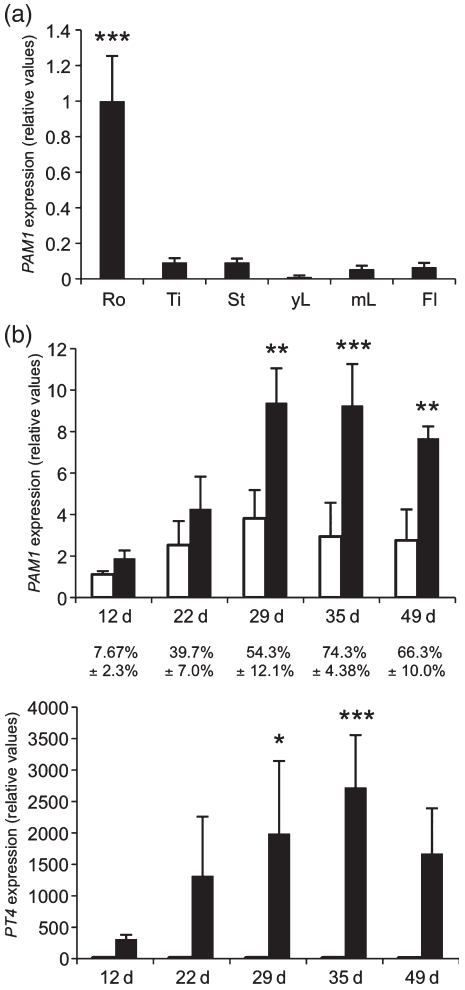

Figure 3. Expression of *PAM1* in various plant organs and in mycorrhizal roots.

(a) The relative mRNA abundance was determined by qRT-PCR. *PAM1* was expressed at the highest levels in roots (Ro), and at lower levels in aerial plant parts such as shoot tips (Ti), stems (St), young leaves (yL), mature leaves (mL) and flowers (Fl). *PAM1* expression is expressed relative to *GAPDH* expression and normalized to one in roots. Expression in roots was significantly higher than in all aerial tissues.

(b) Expression of *PAM1* (top) and *PT4* (bottom) in mycorrhizal roots. Plants in pot cultures were inoculated with *Glomus intraradices* (black columns) or not (white columns), and were then sampled after 12, 22, 29, 35 and 49 days. Expression levels are given relative to *GAPDH* expression and are normalized to one in control roots at 12 days. Statistically different expression levels between mycorrhizal and mock-inoculated roots are marked with asterisks (*0.05 > *P* > 0.01; **0.01 > *P* > 0.002; ***$P < 0.002$). The percentage of root colonization is indicated below the respective columns in (b). Colonization levels and gene expression were determined in three biological replicates. Error bars represent standard deviations of the mean.

low autofluorescence in the green channel (compare Figure 4e,f). These correspond to active arbuscules preceding the onset of senescence (Harrison *et al.*, 2002; Vierheilig, 2004). In contrast, cells that contained arbuscules with elevated green autofluorescence, decreased branching, and clumped appearance exhibited low levels of *PAM1* expression. A similar correlation of gene expression with active arbuscules was found for *MtPT4* (Harrison *et al.*, 2002). The parallel induction of *PAM1* and *PT4* during AM development in our experiments (Figure 3b) is in agreement with this observation.

Subcellular localization of PAM1-GFP fusions

The predicted PAM1 protein carries neither a recognizable signal peptide nor any organellar targeting sequence. However, the presence of an MSP domain and an ankyrin domain suggests that PAM1 may interact with membranes or with the cytoskeleton (Bennett and Baines, 2001; Lev *et al.*, 2008). In order to investigate its subcellular localization, PAM1 was fused in frame to GFP at the N- and C-terminus. The former fusion protein was expressed under the control of the cauliflower mosaic viral 35S promoter (Pro35S:GFP-PAM1), whereas the latter was under the control of the endogenous PAM1 promoter (ProPAM1:PAM1-GFP). The constructs were introduced into wild type W115 and *pam1-1* mutants via root transformation with *Agrobacterium rhizogenes*. As both fusion proteins exhibited indistinguishable subcellular localization patterns, only the results with ProPAM1:PAM1-GFP are reported here. PAM1-GFP fusion protein, which complemented arbuscule development in the mutant (Figure 5, compare with Figure 1a–c), was localized throughout the cytoplasm, including transvacuolar cytoplasmic strands, and to the nucleus (Figure 6a–c). In addition, a strong signal was detected in small spherical structures that moved rapidly along the cellular periphery and along cytoplasmic strands (Figure 6a–c; Video Clip S1). This subcellular localization pattern was observed in wild type plants (Figure 6b,c) and in complemented *pam1-1* mutants (Figure 6a,e–h). Free GFP was detected throughout the cytoplasm and the nucleus, but no fluorescent dots were observed (Figure 6d).

To further explore the nature of the fluorescent dots, transgenic roots expressing PAM1-GFP were stained with FM4-64, which marks endosomes (Bolte *et al.*, 2004; Geldner and Jürgens, 2006), and with MitoTracker® Red, which specifically stains mitochondria (Sheahan *et al.*, 2005). However, neither of these fluorescent markers coincided with the PAM1-GFP signal (Figure 6e,f). Upon inoculation with *Glomus intraradices*, the fluorescent dots associated with intracellular hyphae and with developing arbuscules (Figure 6g,h). Notably, in colonized cells the general cytoplasmic signal was weaker than in non-colonized cells, whereas the fluorescent dots appeared more numerous and more intensely stained relative to the surrounding cytoplasm (Figure 6h).

Immunolocalization of PAM1

Based on confocal microscopy, we estimated that the fluorescent dots had a diameter of approximately 1 μm. Transmission electron microscopical (TEM) analysis revealed that membrane-bound spherical structures of a similar size were

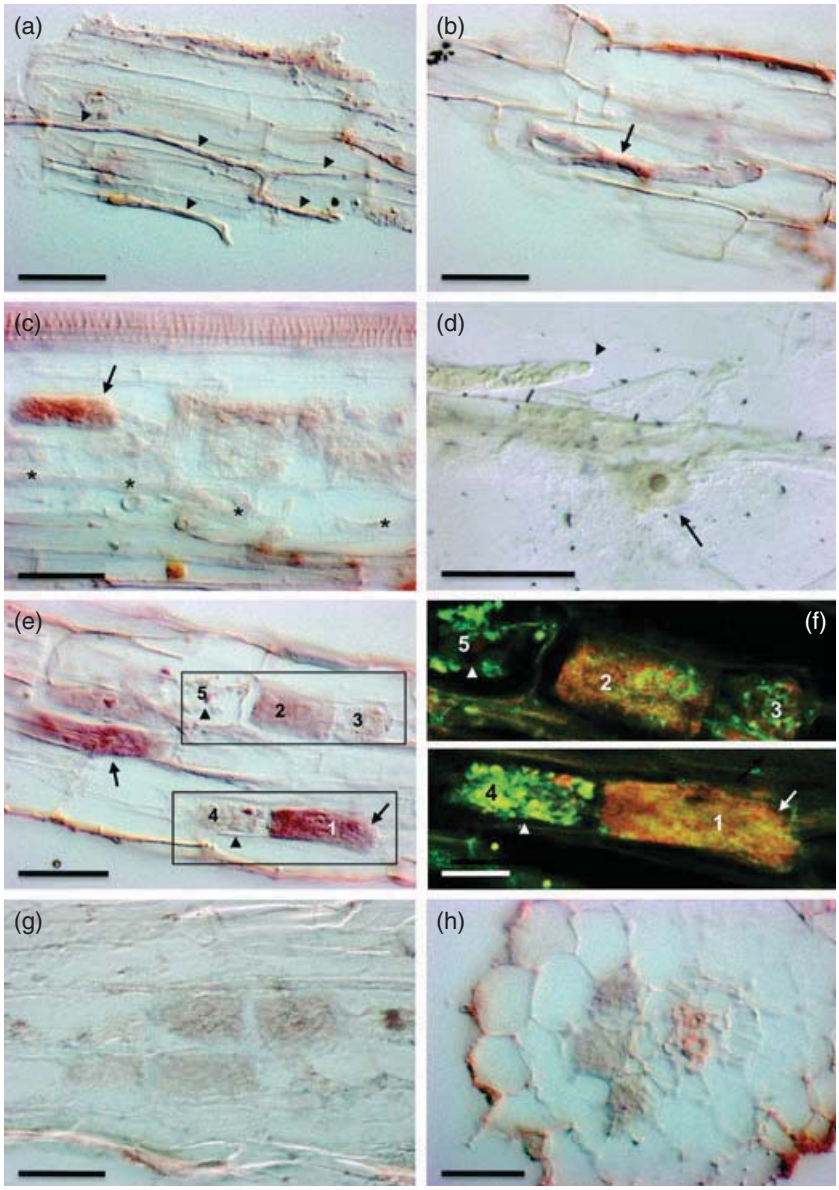

Figure 4. Expression pattern of *PAM1* in mycorrhizal roots as determined by *in situ* hybridization.
(a–e) Hybridized with an antisense probe; (g, h) hybridized with a sense probe; (a–g) longitudinal sections; (h) transverse section.
(a) Roots that carried extraradical hyphae (arrowheads) did not exhibit any signal above background level.
(b) Epidermal cells with a penetration hypha occasionally exhibited a signal around the hypha (arrow).
(c) Cells that were in contact with intercellular hyphae (asterisks) did not express *PAM1* above the background level, whereas in cells with arbuscules, *PAM1* was markedly induced (arrow).
(d) Cortex cell with an adjacent hyphal tip (arrowhead). The nucleus (arrow) is positioned close to the fungal hypha, indicating that the cell may have perceived the presence of the fungus; however, *PAM1* is not induced.
(e) Although some cells with arbuscules exhibited a strong signal (arrows), others had only intermediate signal or were devoid of any staining. The latter frequently contained clumped arbuscules that are likely to represent senescing arbuscules (arrowheads). Numbers, arrowheads and the arrow in the boxed areas correspond to the numbers and arrows in (f).
(f) Boxed areas from (e) were analysed by confocal microscopy. The *in situ* signal in (e) is inversely correlated with the greenish autofluorescence and hyphal clumping in senescing arbuscules. The numbers refer to the arbuscules in (e) and reflect their progressive senescence, with one indicating a fully active arbuscule and five indicating a collapsed arbuscule.
(g, h) Hybridization with a sense probe resulted in a weak background signal.
Scale bars: 50 μm (a–c, e, g, h); 25 μm (d, f).

associated with the vacuolar side of the cytoplasm in colonized cells with arbuscules (Figure 6i), where they were frequently localized to the vicinity of fungal hyphae (arrowheads), as well as in non-infected cells (Figure 6i, inset). Based on their spherical shape, and on their apparent association with the tonoplast, we further refer to them as

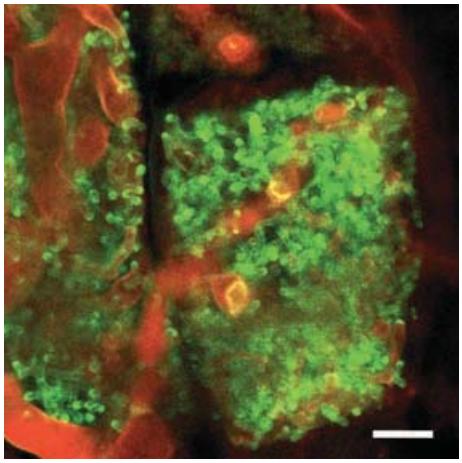

Figure 5. Restored arbuscule development in a complemented *pam1-1* mutant.
After live imaging of GFP (Figure 6g,h), inoculated roots were cleared and stained with wheat germ agglutinin coupled to fluorescein isothiocyanate (FITC, green), which primarily stains the fine branches, and propidium iodide (red), which stains the thick trunk hyphae. Note that the arbuscules are branched as intensely as in the wild type (compare with Figure 1a), and are not truncated, as in the non-transformed *pam1-1* mutant (Figure 1b). Scale bar: 10 μm.

tonospheres. To test whether tonospheres contained PAM1 protein, immunogold localization was performed with affinity-purified antiserum raised against an N-terminal peptide of PAM1 (PLNKIRYSTRPQSG). It should be noted here that, in order to preserve the antigenicity of proteins, the fixation of tissue with osmium tetroxide (OsO_4) had to be omitted, resulting in the limited preservation and contrast of membranes in immunogold experiments. On ultrathin sections of colonized cortical cells, immunogold particles were associated primarily with circular structures of approximately 0.5–1 μm in diameter that occupied a similar position as the tonospheres (Figure 6j, compare with Figure 6i). Omission of the primary PAM1 antibody abolished the signal completely (Figure 6k). These results confirm the results obtained with GFP-tagged PAM1 fusion protein, and indicate that PAM1 is indeed localized to tonospheres. In order to obtain additional confirmation for the membrane association of PAM1, we co-expressed the C-terminal PAM1 fusion (Pro35S:PAM1-GFP) together with free DsRed, as a cytoplasmic reference, in onion epidermal cells. PAM1-GFP co-localized with DsRed in the cytoplasm (Figure 6l), but in addition, PAM1-GFP fusion protein was localized to invaginations of the tonoplast that resembled tonospheres in petunia roots (compare with Figure 6i), although they were larger. Free GFP co-expressed with DsRed showed a perfectly overlapping localization to the cytoplasm, without any association with membranes (data not shown). These results document an inherent affinity of PAM1 to membranes, in particular to a subdomain of the tonoplast.

DISCUSSION

PAM1 is indispensable for arbuscule development

As a result of the strictly biotrophic nature of AM fungi, analysis of potential cortical phenotypes of AM mutants is prevented if fungal colonization is aborted at the level of the epidermis. In this case, inoculation from nearby colonized wild type plants (nurse plants) can help, because hyphae emanating from nurse plants profit from the con-

Figure 6. Subcellular and ultrastructural analysis of PAM1 localization with GFP-tagged PAM1, and with antibodies raised against PAM1 peptide.
(a–h, l) Confocal laser scanning microscopical images of transformed hairy roots (a–h) and onion epidermal cells (l) expressing various GFP constructs. (i–k) Transmission electron microscopic images of colonized roots. (a–h) Transgenic hairy roots of wild type (b–d) and *pam1-1* mutants (a,e–h) expressing a C-terminal PAM1-GFP fusion under the control of the endogenous PAM1 promoter (ProPAM1:PAM1-GFP; a–c, e–h) or free GFP (d). Counterstaining in (a), (b), (g) and (h) was performed with propidium iodide.
(a) In epidermal cells and root hairs, the PAM1-GFP signal was localized to the cytoplasm, the nuclei (n) and accumulated in small spherical structures (arrowheads), which associated with cytoplasmic strands and with the cortical cytoplasm.
(b) Cortical cells exhibited a similar distribution of PAM1-GFP as epidermal cells (cf. panel a).
(c) Close-up of an individual cortical cell showing the association of the PAM1-GFP dots with cytoplasmic strands and with the perinuclear and cortical cytoplasm (cf. Video Clip S1).
(d) Free GFP was localized to the cytoplasm, the nuclei (n) and to cytoplasmic strands (arrowhead). Left: small cortical cells near the root tip. Right: Fully expanded epidermal cell of a differentiated root.
(e) Staining with FM4-64 of cells near the root tip revealed the plasma membrane and numerous small endosomal compartments within the cells. The PAM1-GFP signal did not coincide with endosomes.
(f) PAM1-GFP accumulating dots did not coincide with mitochondria visualized with MitoTracker® Red (red dots).
(g) Complementation of a *pam1* mutant by transformation with ProPAM:PAM1-GFP. Four weeks after inoculation intracellular accommodation and hyphal proliferation in cortical cells was observed (arrows). Many fluorescent dots were associated with hyphae.
(h) Cortical cell of the same root as in (g). Expression of ProPAM:PAM1-GFP promoted arbuscule development (cf. Figure 5). Note that PAM1-GFP dots were particularly prominent in areas with fine hyphal branches (box).
(i) Overview of a cortical cell with a developing arbuscule within the central vacuole. Fine and intermediate hyphal branches (asterisks) can be distinguished by their electron-dense walls. Note the membranous bridges (arrows) that connect patches of plant cytoplasm containing fungal hyphae. Spherical membrane structures (arrowheads), referred to as tonospheres, were frequently positioned next to fungal hyphae. Inset: tonospheres were also found in non-colonized cells.
(j) Immunogold labelling highlights a tonosphere (arrowheads) in a colonized cell (as in panel i).
(k) Section as in (j) that was processed without the primary peptide antibody.
(l) An onion epidermal cell expressing PAM1-GFP together with free DsRed exhibits uniform yellow staining, resulting from the overlay of green and red signal in the cytoplasm. In addition, protrusions of the tonoplast into the vacuolar lumen exhibit PAM1-GFP signal (arrowheads).
Abbreviations: fv, fungal vacuole; nucleus; v, vacuole. Scale bars: 10 μm (a, c–h, l); 50 μm (b); 1 μm (i); 500 nm (j, k).

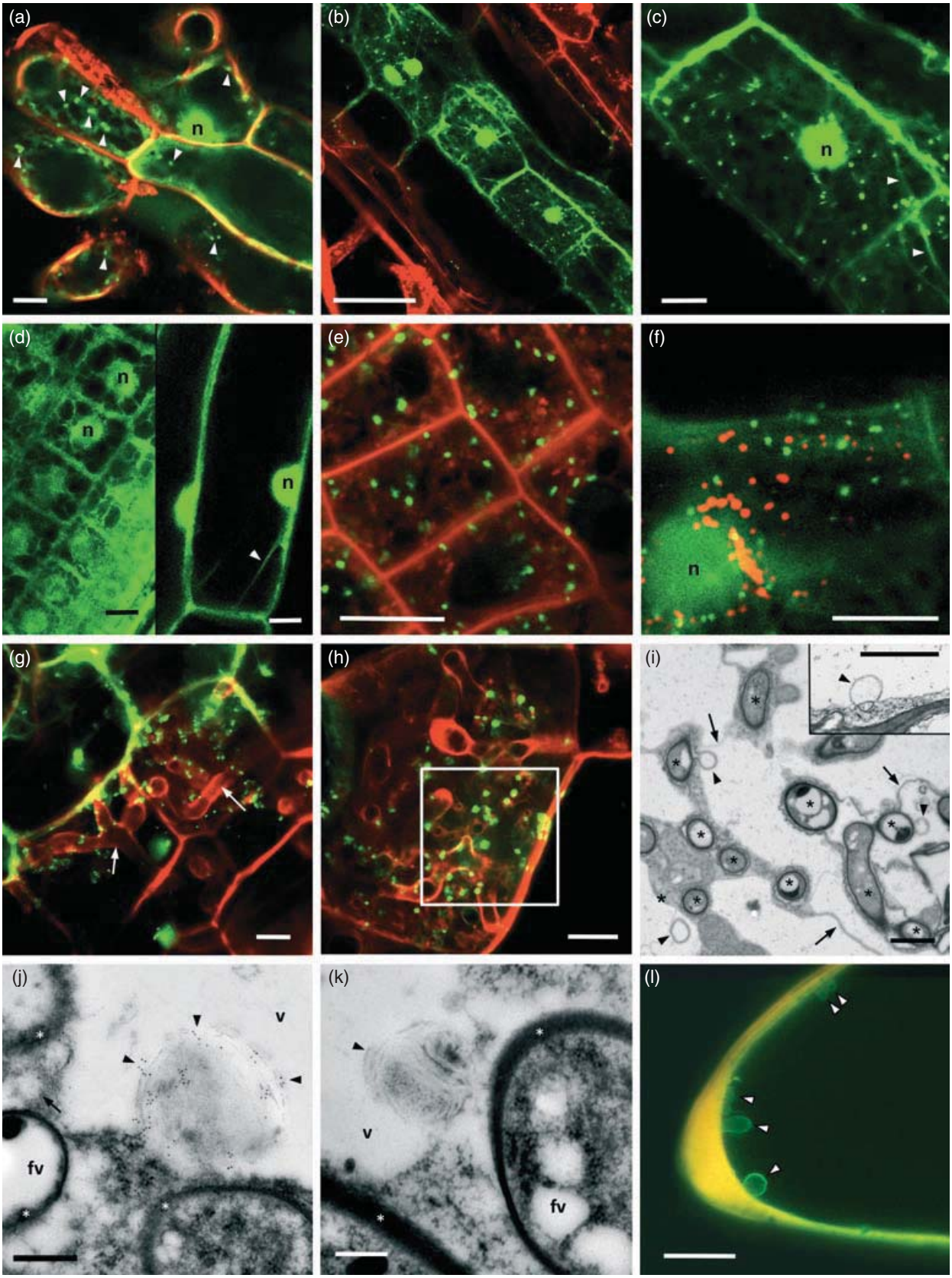

tinuous supply of resources from their host, and hence can potentially overcome the epidermal block and colonize mutant plants even if the interaction is non-functional. Microscopic analysis of *pam1* mutants inoculated with nurse plants showed that overall root colonization was not affected in *pam1*, compared with the wild type, whereas arbuscule development was severely inhibited in both mutant alleles. This shows that *PAM1*, like its homologue in *M. truncatula* (Pumplin *et al.*, 2010), is indispensable for arbuscule differentiation in cortical cells, whereas its function is conditional for epidermal colonization at high infection pressure.

Similarity of the PAM1 ankyrin domain with the membrane-binding domain of animal ankyrins

Like the VAPYRIN of *M. truncatula*, the predicted PAM1 protein consists of an N-terminal MSP domain (also referred to as VAP domain) and an ankyrin domain. However, whereas VAPYRIN has been reported to have eight ankyrin repeats (Pumplin *et al.*, 2010), modelling of the three-dimensional structure of PAM1 predicted eleven repeats. This structure, which is unique among plants, exhibits conspicuous similarity with animal ankyrins (Mosavi *et al.*, 2004), such as human ankyrin R (Michaely *et al.*, 2002; compare with Figure 2d). Because of its association with the plasmalemma, the ankyrin domain of ankyrin R is referrred to as the 'membrane-binding' domain. Membrane association is mediated by the binding of the ankyrin domain to several integral membrane proteins, such as Na/K ATPase, Cl/HCO3 anion exchanger, voltage-gated sodium channel and clathrin heavy chain (Bennett and Baines, 2001; Michaely *et al.*, 2002).

PAM1 marks a membrane-bound subcellular compartment

In view of the similarity with animal ankyrins, the association of PAM1 with a membrane-bound cellular subcompartment is not surprising. The PAM1 homologue VAPYRIN of *M. truncatula* is entirely cytoplasmic in roots, but becomes localized to fluorescent dots in cells colonized by a mycorrhizal fungus (Pumplin *et al.*, 2010). In petunia, however, the GFP-tagged PAM1 (N- or C-terminal fusions) always occurs in both forms, and becomes almost completely confined to fluorescent dots in colonized cortical cells (Figure 6h), as well as in young cells close to the root tip (Figure 6e).

Consistent with GFP localization data, ultrastructural analysis reveals membrane-bound structures associated with the tonoplast, referred to as tonospheres, which are marked with antibodies against PAM1. Additional confirmation of the membrane association of PAM1 comes from expression in onion epidermal cells, in which the tonospheres were larger, and therefore allowed a better resolution of the fluorescently labelled membrane than in petunia roots. Taken together, our data suggest that PAM1 occurs in a soluble cytoplasmic form and in a membrane-bound form. During intracellular accommodation of the mycorrhizal endosymbiont, PAM1 becomes increasingly recruited to tonospheres, which represent a previously unknown subcellular compartment at the interface of cytoplasm and vacuole.

Function of PAM1 in intracellular accommodation and morphogenesis of the AM fungus

Mobile structures with a similarity to tonospheres were observed in Arabidopsis cotyledons (Saito *et al.*, 2002), where they have been hypothesized to contribute to transport and turnover of cellular constituents. As in Arabidopsis, the tonospheres of petunia roots occur constitutively, indicating that they may perform a basic cellular function independent of symbiosis. In colonized cells, PAM1 became increasingly localized to tonospheres, which became associated with areas of intense hyphal branching (Figure 6; Pumplin *et al.*, 2010). Based on the mutant phenotype, PAM1 in tonospheres may be involved in the transport of a component with an essential function during intracellular colonization by AM fungi. For example, tonospheres could function as a mobile reserve of membrane material for the expanding membrane system during arbuscule development. This scenario could explain why *PAM1* function is more critical in cortical cells than in epidermal cells, because the former generate a much more extensive membrane system upon colonization (Pumplin and Harrison, 2009). Alternatively, tonospheres may contain a cargo that is required for fungal growth and/or morphogenesis, in particular for hyphal branching during arbuscule development. For example, tonospheres could represent a subdomain of the vacuole that carries symbiosis-related proteases (Takeda *et al.*, 2007).

PAM1 consists almost entirely of protein–protein interaction domains, and is therefore likey to act in concert with other components. Future experiments should address such interacting proteins, and their role in the intracellular accommodation of endosymbionts. Furthermore, detailed characterization of tonospheres is required to elucidate their role in basic cell biology, and in endosymbiosis.

EXPERIMENTAL PROCEDURES

Plant material, growth conditions, inoculation and quantification of root colonization

Plants were grown in a mixture of sand and soil (2:1, v/v) and inoculated with *Glomus intraradices* (MUCL43204) as described by Sekhara Reddy *et al.* (2007), either in pot cultures (250 ml) with an inoculum consisting of dried soil and roots of well colonized leek, or in compartmented inoculation chambers that were isolated from colonized nurse plants by a double nylon mesh (20-μm mesh width) (Wyss *et al.*, 1991). Plants were fertilized weekly with a basic nutrient solution (Sekhara Reddy *et al.*, 2007). For quantification of colonization, roots were stained with trypan blue and spread horizontally over microscope slides with a regular pattern of vertical

yellow stripes (for details see Sekhara Reddy *et al.*, 2007). Per sample, 100 intersections of roots with the yellow stripes were examined for the presence of fungal structures. The significance of differences was tested by ANOVA followed by Tukey's honestly significant difference (HSD) test in the statistical software R v2.9.1 (R Development Core Team, 2009).

Isolation of *PAM1*

DNA isolation and manipulation was carried out according to Stuurman *et al.* (2002). Transposon display was carried out as described by Van den Broeck *et al.* (1998), with minor modifications. Briefly, DNA of mutant and wild type plants of a segregating population of *pam1-2* was restriction digested with *Bfa*I and *Mun*I, and ligated to adapters. A first PCR amplified all fragments with adapter primers, and a second nested PCR with adapter primer and radiolabelled transposon primer (IR primer) amplified flanking sequences of transposon insertions. Both primers had a single nucleotide extension to reduce the number of amplified fragments to 1/16, thereby decreasing the complexity of the reaction, and improving the resolution and signal strength in subsequent steps. Amplicons were resolved by polyacrylamide gel electrophoresis and revealed by autoradiography with Kodak Biomax film (Sigma-Aldrich, http://www.sigmaaldrich.com). An amplicon that co-segregated with the mutant phenotype was identified with the primer combination IR + G and *Mse*I + C. The band was extracted from the gel, cloned into pGEM-T Easy (Promega, http://www.promega.com) and sequenced. Genomic sequences of the transcribed region of wild type petunia (line W115), of the *pam1-1* allele, of a revertant allele and of a 1674-bp fragment upstream of the predicted start codon were isolated using the Universal GenomeWalker kit (Clontech, http://www.clontech.com) according to the supplier's recommendations. The cDNA sequence of the wild type *PAM1* gene was isolated by RACE PCR using the SMART RACE cDNA Amplification kit (Clontech). See Appendix S1 for the modelling of the three-dimensional structure of PAM1.

Gene expression analysis

RNA isolation was carried out as described by Sekhara Reddy *et al.* (2007) using the hot phenol method, or with the RNeasy kit (Qiagen, http://www.qiagen.com). First-strand cDNA synthesis was performed with the Omniscript RT kit or the Quantitect RT kit (both Qiagen), according to the manufacturer's guidelines. qRT-PCR was carried out with the ABsolute qPCR SYBR Green mastermix (Thermo Scientific, http://www.thermo.com) in a Rotorgene thermocycler (Corbett Life Science, http://www.corbettlifescience.com) with the following primers:

PAM1-N-F, 5′-CACTTTAGACATGGTTCCAAGTGATTG-3′; PAM1-N-R, 5′-TAGCCAAGTGTAACAAAGTTTGACCTTC-3′; PAM1-C-F, 5′-AGCTAGCATCAATGGACGTGATCA-3′; PAM1-C-R, 5′-GACCAGATTCCACTGCACAATG-3′; PhPT4-F7, 5′-TTGATGAATTTTGAAGGTAAACCATTTAACGTG-3′; PhPT4-R7, 5′-AGTGTTGGCTTTGCTAGTAAGTCCCATAAC-3′; PhGAPDH-F3, 5′-GGAATCAACGGTTTTGGAAGAATTGGGCG-3′; PhGAPDH-R4, 5′-GGCCGTGGACACTGTCATACTTGAACA-3′; PAM1-N-F and PAM1-N-R amplify a sequence of 221 bp starting at position 320 from the start codon, whereas PAM1-C-F and PAM1-C-R amplify a sequence of 164 bp starting at position 1349 from the start codon. Gene expression levels are expressed relative to GAPDH (Sekhara Reddy *et al.*, 2007). Each expression value represents the average of triplicate measurements from RNA samples extracted independently from three biological replicates. Error bars represent the standard deviation of the means. Differences between expression levels in time were analysed by ANOVA followed by Tukey's HSD test. All analyses were carried out in the statistical software R v2.9.1 (R Development Core Team, 2009).

Generation of *GFP-PAM1* fusion constructs and plant transformation

Transformation vectors for subcellular localization of PAM1 were generated as follows: full-length *PAM1* was amplified from cDNA using Gateway-compatible primers, and was directionally cloned into pENTR11 (Invitrogen, http://www.invitrogen.com). An LR-recombinase reaction with the vector pB7WGF2 (http://www.psb.ugent.be) generated a C-terminal in-frame fusion of PAM1 with GFP under the control of the cauliflower mosaic viral 35S promoter (Pro35S:GFP-PAM1). Another LR reaction with pK7FWG2_RR (vector includes dsRed as cytosolic marker) gave the Pro35S:PAM1-GFP construct. For the generation of the ProPAM1:PAM1-GFP construct, a 1674-bp sequence upstream of the *PAM1* start codon was cloned into pGEM-T Easy. Using Gateway-compatible primers, ProPAM1 was amplified by PCR from plasmid DNA and introduced into pDONR201 by a BP-recombinase reaction. A subsequent LR reaction with pHGWFS7 (http://www.psb.ugent.be) generated the transformation vector, pHProPAM1FS7. The complete *PAM1* cDNA was amplified with primers containing *Xho*I sites at each end, and cloned into the transformation vector downstream of the PAM1 promoter, and in frame with GFP. Vectors were amplified in *Escherichia coli* TOP10 cells and used for *Agrobacterium rhizogenes*-mediated transformation of petunia roots as described by Boisson-Dernier *et al.* (2001). Biolistic transfection of onion epidermal cells was carried out as described by Ibrahim *et al.* (2000).

In situ hybridization

To generate probes for *in situ* hybridization, full-length *PAM1* was cloned into pGEM-T Easy vector (Promega). Digoxigenin-labelled sense and antisense RNA probes were synthesized with T7 and SP6 RNA polymerase using the DIG RNA labelling kit (Roche, http://www.roche.com) according to the guidelines of the provider. Fixation, embedding, sectioning and hybridization were carried out as described by Langdale (1993). Briefly, root segments of 5 mm in length were fixed in 4% paraformaldehyde in PBS overnight at 4°C. The tissue was then dehydrated in a graded ethanol series and subsequently in Histoclear (National Diagnostics, http://www.nationaldiagnostics.com). Finally, root pieces were embedded in Paraplast (Sigma-Aldrich), sectioned to 14-μm thickness on a rotary microtome (Leitz, http://www.leitz.com) and mounted on Superfrost Plus slides (Menzel, http://www.menzel.de). *In situ* hybridization was performed as described by Langdale (1993). Alkaline phosphatase activity of anti-digoxigenin-alkaline phosphatase conjugate (Roche) was detected with Western Blue (Promega).

Immunolocalization

Peptide design (PLNKIRYSTRPQSG), synthesis and raising of antiserum in rabbits, was carried out by GenScript (http://www.genscript.com). Antiserum was affinity purified using Affigel10 according to the manufacturer's guidelines. Briefly, 4 mg of peptide was coupled to 5 ml Affigel10 in 10 mM 3-(*N*-morpholino) propanesulphonic acid (MOPS) pH = 7.3 at 4°C overnight. After washing, the column was blocked with 1 M ethanolamine, pH 8.0, for 30 min. Antiserum was heated to 56°C to inactivate the complement factors. Following centrifugation (5 min at 5000 ***g***), 0.8 ml antiserum was incubated with 0.4 ml coupled affinity beads overnight at 4°C. After transfer to syringes and extensive washing with 1 M NaCl, affinity-bound material was eluted with 20 mM HCl into 100 μl of 1 M Tris–Cl, pH = 8.0, for neutralization.

Transmission electron microscopic analysis was performed as described by Sieber *et al.* (2000). Briefly, root segments were fixed in 2% glutaraldehyde in 0.1 M Na-cacodylate buffer pH = 7.4, and postfixed with 1% OsO_4 in the same buffer, followed by embedding in Spurr's standard epoxy resin (Spurr, 1969) and sectioning (75 nm). For immunocytochemical analysis, OsO_4 was omitted, and the samples were embedded in LRwhite resin (Fluka, avalaible from Sigma-Aldrich). After sectioning, the mounted ultrathin sections were processed as described by Sieber *et al.* (2000). Briefly, sections were blocked with goat serum and incubated with the anti-PAM1 antibody (1:10), followed by treatment with the secondary antibody (goat-anti-rabbit) coupled to colloidal gold (BioCell, http://www.biocell.com). For the control treatment, the primary antibody was omitted.

Microscopy

For phenotypic characterization, colonized roots were cleared with 10% KOH at 95°C for 20 min, followed by rinsing and staining with 0.1% acid fuchsin in 30% lactic acid for 3 days at room temperature (25°C). Fungal staining with wheat germ agglutinin coupled to fluorescein isothiocyanate (WGA-FITC; Sigma-Aldrich) was performed by clearing with KOH (see above), followed by fixation with 4% formaldehyde, staining with 50 μg ml^{-1} WGA-FITC in Sörensen buffer, and counterstaining with 25 μg ml^{-1} propidium iodide in 20 mM Tris–Cl, pH = 7.5. For the staining of mitochondria and endosomes, 0.2 μM MitoTracker® Red and 10 μM FM4-64 (both from Molecular Probes, available from Invitrogen) were used in distilled water, respectively. Confocal laser scanning microscopy was performed on a Leica SP5. Electron microscopic analysis was performed on a Philips CM 100 BIOTWIN equipped with a Morada side-mounted digital camera (Olympus, http://soft-imaging.net) for image acquisition.

ACKNOWLEDGEMENTS

We thank Sven Bacher for statistical analysis. This work was supported by the Swiss National Science Foundation (grant nos 3100AO-101792/1 and 3100AO-118055).

SUPPLEMENTARY INFORMATION

Additional Supporting Information may be found in the online version of this article:

Video Clip S1. Movement of tonospheres in a cortical cell expressing ProPAM1:PAM1-GFP.

Appendix S1. Supporting experimental procedures: 3D modelling of the MSP domain and the ankyrin domain of PAM1.

REFERENCES

Bennett, V. and Baines, A.J. (2001) Spectrin and ankyrin-based pathways: metazoan inventions for integrating cells into tissues. *Physiol. Rev.* **81**, 1353–1392.

Blancaflor, E.B., Zhao, L.M. and Harrison, M.J. (2001) Microtubule organization in root cells of *Medicago truncatula* during development of an arbuscular mycorrhizal symbiosis with *Glomus versiforme*. *Protoplasma*, **217**, 154–165.

Boisson-Dernier, A., Chabaud, M., Garcia, F., Becard, G., Rosenberg, C. and Barker, D.G. (2001) Agrobacterium rhizogenes-transformed roots of *Medicago truncatula* for the study of nitrogen-fixing and endomycorrhizal symbiotic associations. *Mol. Plant Microbe Interact.* **14**, 695–700.

Bolte, S., Talbot, C., Boutte, Y., Catrice, O., Read, N.D. and Satiat-Jeunemaitre, B. (2004) FM-dyes as experimental probes for dissecting vesicle trafficking in living plant cells. *J. Microsc.* **214**, 159–173.

Bonfante-Fasolo, P. (1984) Anatomy and morphology of VA mycorrhizae. In *VA Mycorrhizae* (Powell, C.L. and Bagyaraj, D.J., eds). Boca Raton, FL, USA: CRC Press, pp. 5–33.

Bucher, M. (2007) Functional biology of plant phosphate uptake at root and mycorrhiza interfaces. *New Phytol.* **173**, 11–26.

Geldner, N. and Jürgens, G. (2006) Endocytosis in signalling and development. *Curr. Opin. Plant Biol.* **9**, 589–594.

Genre, A. and Bonfante, P. (1998) Actin versus tubulin configuration in arbuscule-containing cells from mycorrhizal tobacco roots. *New Phytol.* **140**, 745–752.

Genre, A. and Bonfante, P. (1999) Cytoskeleton-related proteins in tobacco mycorrhizal cells: gamma-tubulin and clathrin localisation. *Eur. J. Histochem.* **43**, 105–111.

Genre, A., Chabaud, M., Timmers, T., Bonfante, P. and Barker, D.G. (2005) Arbuscular mycorrhizal fungi elicit a novel intracellular apparatus in *Medicago truncatula* root epidermal cells before infection. *Plant Cell*, **17**, 3489–3499.

Genre, A., Chabaud, M., Faccio, A., Barker, D.G. and Bonfante, P. (2008) Prepenetration apparatus assembly precedes and predicts the colonization patterns of arbuscular mycorrhizal fungi within the root cortex of both *Medicago truncatula* and *Daucus carota*. *Plant Cell*, **20**, 1407–1420.

Gerats, A.G.M., Huits, H., Vrijlandt, E., Maraña, C., Souer, E. and Beld, M. (1990) Molecular characterization of a nonautonomous transposable element (dTph1) of petunia. *Plant Cell*, **2**, 1121–1128.

Gutjahr, C., Banba, M., Croset, V., An, K., Miyao, A., An, G., Hirochika, H., Imaizumi-Anraku, H. and Paszkowski, U. (2008) Arbuscular mycorrhiza-specific signaling in rice transcends the common symbiosis signaling pathway. *Plant Cell*, **20**, 2989–3005.

Harrison, M.J., Dewbre, G.R. and Liu, J.Y. (2002) A phosphate transporter from *Medicago truncatula* involved in the acquisiton of phosphate released by arbuscular mycorrhizal fungi. *Plant Cell*, **14**, 2413–2429.

Ibrahim, M., Si-Ammour, A., Celio, M.R., Mauch, F. and Menoud, P.A. (2000) Construction and application of a microprojectile system for the transfection of organotypic brain slices. *J. Neurosci. Methods*, **101**, 171–179.

Langdale, J. (1993) In situ hybridization. In *The Maize Handbook* (Freeling, M. and Walbot, V., eds). Berlin: Springer Verlag, pp. 165–180.

Laurent, F., Labesse, G. and de Wit, P. (2000) Molecular cloning and partial characterization of a plant VAP33 homologue with a major sperm protein domain. *Biochem. Biophys. Res. Commun.* **270**, 286–292.

Lev, S., Ben Halevy, D., Peretti, D. and Dahan, N. (2008) The VAP protein family: from cellular functions to motor neuron disease. *Trends Cell Biol.* **18**, 282–290.

Markmann, K., Giczey, G. and Parniske, M. (2008) Functional adaptation of a plant receptor-kinase paved the way for the evolution of intracellular root symbioses with bacteria. *PLoS Biol.* **6**, 497–506.

Michaely, P., Tomchick, D.R., Machius, M. and Anderson, R.G.W. (2002) Crystal structure of a 12 ANK repeat stack from human ankyrinR. *EMBO J.* **21**, 6387–6396.

Mosavi, L.K., Cammett, T.J., Desrosiers, D.C. and Peng, Z.Y. (2004) The ankyrin repeat as molecular architecture for protein recognition. *Protein Sci.* **13**, 1435–1448.

Oldroyd, G.E.D. and Downie, J.A. (2006) Nuclear calcium changes at the core of symbiosis signalling. *Curr. Opin. Plant Biol.* **9**, 351–357.

Oldroyd, G.E.D., Harrison, M.J. and Paszkowski, U. (2009) Reprogramming plant cells for endosymbiosis. *Science*, **324**, 753–754.

Parniske, M. (2008) Arbuscular mycorrhiza: the mother of plant root endosymbioses. *Nat. Rev. Microbiol.* **6**, 763–775.

Pumplin, N. and Harrison, M.J. (2009) Live-cell imaging reveals periarbuscular membrane domains and organelle location in *Medicago truncatula* roots during arbuscular mycorrhizal symbiosis. *Plant Physiol.* **151**, 809–819.

Pumplin, N., Mondo, S.J., Topp, S., Starker, C.G., Gantt, J.S. and Harrison, M.J. (2010) *Medicago truncatula* Vapyrin is a novel protein required for arbuscular mycorrhizal symbiosis. *Plant J.* **61**, 482–494.

R Development Core Team (2009) *R: A Language and Environment for Statistical Computing*. Vienna: R Foundation for Statistical Computing.

Saito, C., Ueda, T., Abe, H., Wada, Y., Kuroiwa, T., Hisada, A., Furuya, M. and Nakano, A. (2002) A complex and mobile structure forms a distinct

subregion within the continuous vacuolar membrane in young cotyledons of Arabidopsis. *Plant J.* **29**, 245–255.

Sekhara Reddy, D.M.R., Schorderet, M., Feller, U. and Reinhardt, D. (2007) A petunia mutant affected in intracellular accommodation and morphogenesis of arbuscular mycorrhizal fungi. *Plant J.* **51**, 739–750.

Sheahan, M.B., McCurdy, D.W. and Rose, R.J. (2005) Mitochondria as a connected population: ensuring continuity of the mitochondrial genome during plant cell dedifferentiation through massive mitochondrial fusion. *Plant J.* **44**, 744–755.

Sieber, P., Schorderet, M., Ryser, U., Buchala, A.J., Kolattukudy, P., Metraux, J.P. and Nawrath, C. (2000) Transgenic Arabidopsis plants expressing a fungal cutinase show alterations in the structure and properties of the cuticle and postgenital organ fusions. *Plant Cell*, **12**, 721–737.

Spurr, A.R. (1969) A low-viscosity epoxy resin embedding medium for electron microscopy. *J. Ultrastruct. Res.* **26**, 31–43.

Stuurman, J., Jäggi, F. and Kuhlemeier, C. (2002) Shoot meristem maintenance is controlled by a GRAS-gene mediated signal from differentiating cells. *Genes Dev.* **16**, 2213–2218.

Takeda, N., Kistner, C., Kosuta, S., Winzer, T., Pitzschke, A., Groth, M., Sato, S., Kaneko, T., Tabata, S. and Parniske, M. (2007) Proteases in plant root symbiosis. *Phytochemistry*, **68**, 111–121.

Van den Broeck, D., Maes, T., Sauer, M., Zethof, J., De Keukeleire, P., D'Hauw, M., Van Montagu, M. and Gerats, T. (1998) Transposon display identifies individual transposable elements in high copy number lines. *Plant J.* **13**, 121–129.

Vierheilig, H. (2004) Regulatory mechanisms during the plant-arbuscular mycorrhizal fungus interaction. *Can. J. Bot.* **82**, 1166–1176.

Wegmüller, S., Svistoonoff, S., Reinhardt, D., Stuurman, J., Amrhein, N. and Bucher, M. (2008) A transgenic dTph1 insertional mutagenesis system for forward genetics in mycorrhizal phosphate transport of Petunia. *Plant J.* **54**, 1115–1127.

Wyss, P., Boller, T. and Wiemken, A. (1991) Phytoalexin response is elicited by a pathogen (*Rhizoctonia solani*) but not by a mycorrhizal fungus (*Glomus mosseae*) in soybean roots. *Experientia*, **47**, 395–399.

Accession number of PAM1: FJ717417.1.